1967

XI 2
XII.1

SATURN BASE HEATING REVIEW

Wilson, Homer B

Summary-Abstract

The Saturn I booster which is powered by a cluster of eight rocket engines has been successfully flown on four successive flights. The early success of this large launch vehicle is a strong indication of the soundness of its base heating program. This paper summarizes the thinking that went into the design of our base configuration. Flight test results indicate that pressures, temperatures and heating rates were generally as expected.

New techniques have been investigated for generating design data. It has been found experimentally that pressure and thermal fields establish themselves in one to three milliseconds and that data from the "short duration" technique compare favorably with "long duration" type tests. As a result, the new "short duration" technique has become the standard for generating design data for the Saturn vehicle.

Sat. Tech. Supp.
Aero. & Space Envir.

INTRODUCTION

The first stage of the Saturn I vehicle is powered by 8 liquid oxygen-kerosene motors, each having a thrust of 188,000 pounds giving a total of approximately 1.5 million pounds thrust. It is being developed by MSFC. This vehicle with dummy upper stages has been successfully flown in its first four flights. This paper will present an outline of the thinking that went into the design of the base configuration; present some typical flight results from the first four flights; and show some of our work or work we have sponsored aimed at improving the techniques for generating design data.

S-I STAGE DESIGN

When the design of the Saturn engine cluster began in 1958, the memory of the high base heating rates experienced in the Jupiter and other missile programs was freshly in mind, and attention was immediately focused on this problem. The initial engine configuration proposed by the structural and propulsion designers foresaw, of course, a circular engine arrangement. It was anticipated, however, that this circular arrangement would cause a pronounced recirculation of hot combustion products on the inside of the engine circle, as well as high radiative heat inputs in the same area. This reasoning was later confirmed by the Polaris experience.

Our design was as follows. (Figure 1) We selected a cross-shaped configuration which would permit a minimum of trapped areas. We clustered four engines as closely together as possible in the center to minimize the region of high heating at high altitude. The four other engines were placed as far away as possible to minimize interference at high altitude. A "flame shield" was placed in the plane of the exit of the center engines to protect this area from high convective heating. Another shield, "heat shield", was placed in the plane of the throat of the engines. Flexible curtains fit around the outer engines to permit them to gimbal.

The turbine exhaust was dumped overboard through four outboard ducts from the four inboard engines which are fixed. The overboard duct is believed to be superior to the exhausterator. However, because of the difficulty experienced in the design of a flexible coupling to withstand the high temperatures of the turbine exhaust gases, we accepted the exhausterator for the four outboard or movable engines. Shroud and valley scoops were incorporated to keep the base flushed of combustible mixtures.

The Saturn I booster has now been flown completely successfully on four successive flights. The data obtained from these flights verified our design concepts. A review of some typical flight test data follows.

Comparison of Trajectories

Figure 2 presents a comparison of the trajectories for the first four Saturn flights, SA-1, SA-2, SA-3, and SA-4, all of which were completely successful. The upper portion of the figure presents velocity as a function of time whereas the lower portion of the curve presents altitude versus time. The trajectories flown by SA-1, 2, and 4 are very nearly the same, so we shall use data from these flights for our discussion.

Typical Flight Test Data

Flame Shield Pressures - Figure 3 shows some typical data from flame shield measurements. The pressure shows a decrease with increasing altitude to time of approximately 85 sec. after which the pressure becomes constant which indicates that choking has occurred between the inboard four engines. The pressure remains constant until inboard cut-off occurs. Ambient pressure (noted by the dashed line) is somewhat higher than flame shield pressure due to the pumping action of the jets to approximately 61 seconds. At approximately 61 seconds, reversed flow begins and the flame shield pressure becomes larger than ambient pressure. Reverse flow increases in intensity until approximately 85 seconds at which time choking occurs.

Heat Shield Pressures - Some typical base pressure versus flight time, altitude, and Mach number is shown in figure 4. These data show that the base pressure (average over the whole base) is approximately equal to ambient pressure to a Mach number of about 1.6. For Mach numbers greater than about 1.6, the base pressure becomes larger than ambient, which results from ballooning of the jets at the lower ambient pressures. The difference between the flight data at Mach numbers of about 1.6 and greater is largely due to gage inaccuracy. The gage is a 0 to 20 psi gage to $\pm$ 2 percent or .4 psi accuracy. Figure 5 presents the ratio of flame shield pressure to base pressure. In the earlier part of the flight, the flame shield pressure is smaller than base pressure indicating flow into the flame shield region. At an altitude of about 8 to 12 km, flame shield pressures become larger than base pressures indicating outflow from the flame shield to base area. With increasing altitude, and decreasing base pressure, the ratio of flame shield pressure continues to increase due to decreasing base pressure. The flame shield pressure is constant after choking.

Typical Temperature Data from Flight Test

Flame Shield Gas Temperatures - Figure 6 presents the approximate flame shield temperatures as a function of altitude, time, and Mach number. Flame shield temperatures increase with increasing altitude, reach a peak, decline slightly and then become constant approximately at the point where choking occurs on the flame shield. The temperatures seem to level off at 3100 ^{O}R which is slightly less than one-half of the theoretical chamber temperature. This is due to the fact that the mass reversed into the base area has passed along the cooled walls of the nozzle. Model tests generally indicate temperatures of 1/3 to 1/2 of chamber temperatures, but the nozzle wall temperatures in model tests are usually smaller than that of the prototype. The overshoot of temperatures before choking is typical of that measured in some model tests. Although most model tests also indicate an overshoot in pressure as well, the pressure data measured in our flight tests did not appear to indicate a similar overshoot.

Base Shield Temperatures - Some typical gas temperature distributions about the base of the vehicle are shown in figure 7. The area in the vicinity of the shroud scoops (Area A) indicates the lowest due to the efficient scooping of the shroud scoops. Temperatures in Area B are the next highest because the valley scoops provide somewhat less scooping efficiency. Area C is perhaps the least flushed of all areas and indicated the largest temperatures. Temperatures in Area C are as high as 950 °C and as low as 250 °C in Area A.

Heating Rate Data on Heat Shield - Figure 8 shows some typical heating rate data from the early Saturn flights. The dashed line indicates radiative flux and the solid line indicates total heat flux. During the early part of the flight, the heating is predominantly radiative. From lift-off to about 6 km, we seem to get convective cooling in the base area. For altitudes above 6 km, the results seem to indicate convective heating for the remainder of the flight.

(Short Movie of Saturn Flight not to Exceed 5 Minutes)

Recent Developments in Model Testing

Since little can be accomplished analytically, we have to depend on previous experience, model, and ground tests to generate design data. The initial base heating model tests were made with the "long duration" type test. By "long type tests" we mean that we scale the rocket engine to a model (1/15 to 1/50 scale) for vacuum tank and wind tunnel testing. This type of testing has several disadvantages: (1) the small scale engines have throat heating problems, (2) the model and instrumentation must have high temperatures, and (3) this type of test is costly. Because of these and other disadvantages, we explored short duration shock tube type testing through a contract with Cornell Aeronautical Laboratory.

In the short duration technique, the products of combustion are generated in what we refer to as the constant pressure combustor as shown in figure 9. The fuel, hydrogen or ethene, if we are simulating RP are loaded in one tube and the gaseous oxygen is loaded in the other tube. The fuel and oxygen are retained by diaphragms at the ends of the tubes.

When the diaphragms are ruptured, the fuel and oxygen are mixed just down stream of the mixer plate and burned. Ignition is by means of a spark plug mounted in an ignition tube. The combustor is mounted in a vacuum tank for high altitude testing or in a wind tunnel with ambient flow. The combustor mounted for vacuum tank testing is shown in figure 10. The combustor enclosed in a shroud to simulate the S-I forebody is shown in figure 10a. Figure 10b shows the base of the model mounted in the Cornell 8 x 8 foot Transonic Tunnel.

Some typical data obtained with the short duration technique is shown in figure 11. These data were taken with Saturn 8-engine configuration in the Cornell 8 x 8 foot tunnel at an altitude of 35,000 ft. and Mach number of 1.2. In the lower left hand corner, chamber, flame shield, and base pressures are plotted as a function of time. The chamber pressure is constant after about 2 milliseconds and remains constant for more than 12 milliseconds. We see that by 3 milliseconds both the base and flame shield pressures are constant and remain constant for 8 to 10 milliseconds. In the upper right hand corner, the temperature for the thin film heat transfer gages is plotted as a function of time for gages located on both the flame and heat shields. The initial peak in the temperature curves is caused by the luminous wave from initial combustion. These temperatures are actually surface temperature as a function of time for a semi-infinite slab of material. Heating rates as a function of time are plotted in the lower curves. From these data, it is seen that the initial luminous wave causes a large radiative input. After the luminous wave passes, the heat flux becomes constant at about 4 milliseconds and remains constant for more than 8 milliseconds. These heating rate data indicate that the thermal field has established itself and that we have a few milliseconds in which to make our heat transfer measurements.

The variation of the total radiative and convective heat flux with time is shown in the figure 12. The lower curve represents the convective flux of about 3 BTU/ft^2-sec; the next curve is the radiative flux of the order of approximately 9 BTU/ft^2-sec; and the sum of radiative and convective flux is shown by the upper curve (12 BTU/ft^2-sec).

A comparison of results from short duration technique with long duration type tests and some limited flight tests is shown in the next series of figures. The ratio of flame shield to ambient pressure is shown in figure 13. The short duration (Cornell results) are compared with results from AEDC, Lewis Research Center and some limited flight test data. The comparison is quite good. Figure 14 presents a comparison of the ratio of base to ambient pressure. The short duration results compare reasonably with corresponding long duration test results. The model results are somewhat lower than the flight results in the transonic and low supersonic regime because the scoops were incorrectly scaled. The ratio of boundary layer thickness to scoop height was somewhat larger for the models than for the flight vehicles.

The next figure (15) gives a comparison of heating rates measured from the various facilities. The radiative flux is noted with a flag and a dashed line represents the general variation of the radiative flux with altitude. It is seen that the radiative flux from the various facilities compares quite well. The solid line represents the variation of total heating with altitude. The agreement between total heating is not nearly as good as was the radiative heating, but for this type of test, the agreement is considered good.

In conclusion, the agreement between the two techniques is quite good. The short duration type test has replaced the old long duration type test in the Saturn program.

SA-I BASE CONFIGURATION

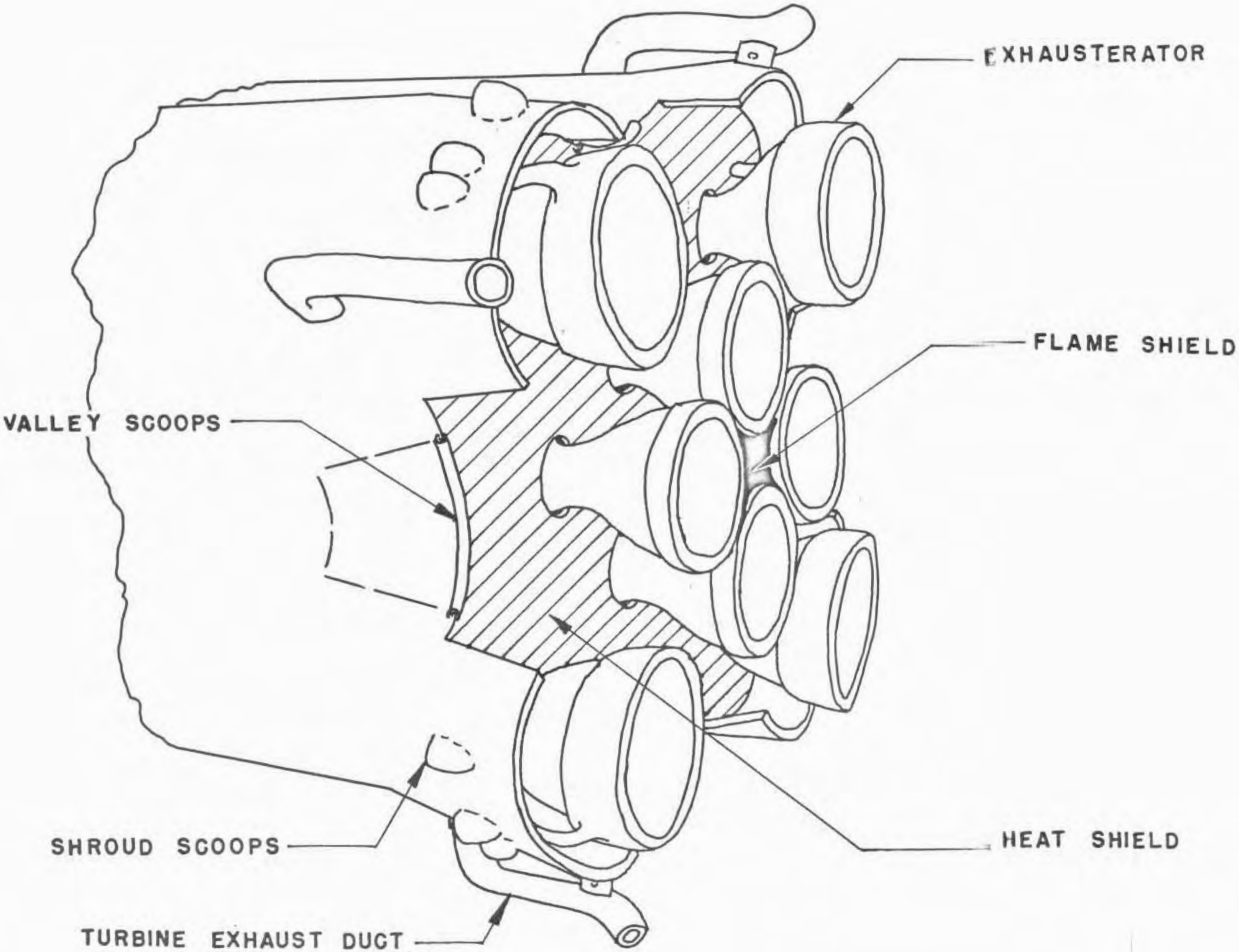

FIGURE I

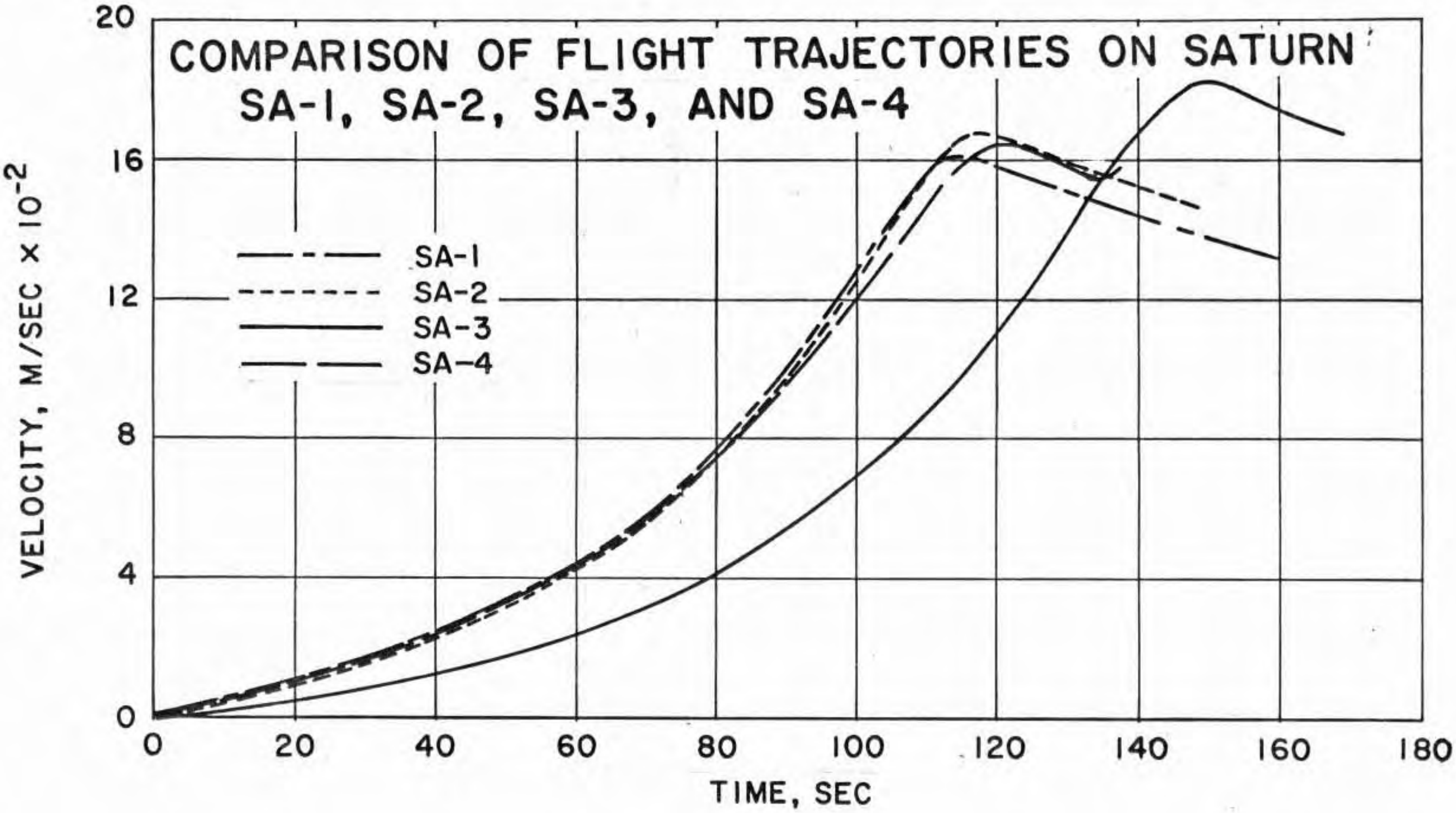
COMPARISON OF FLIGHT TRAJECTORIES ON SATURN
SA-1, SA-2, SA-3, AND SA-4
VELOCITY, M/SEC × 10^{-2}
TIME, SEC
SA-1
SA-2
SA-3
SA-4
0
4
8
12
16
20
0
20
40
60
80
100
120
140
160
180

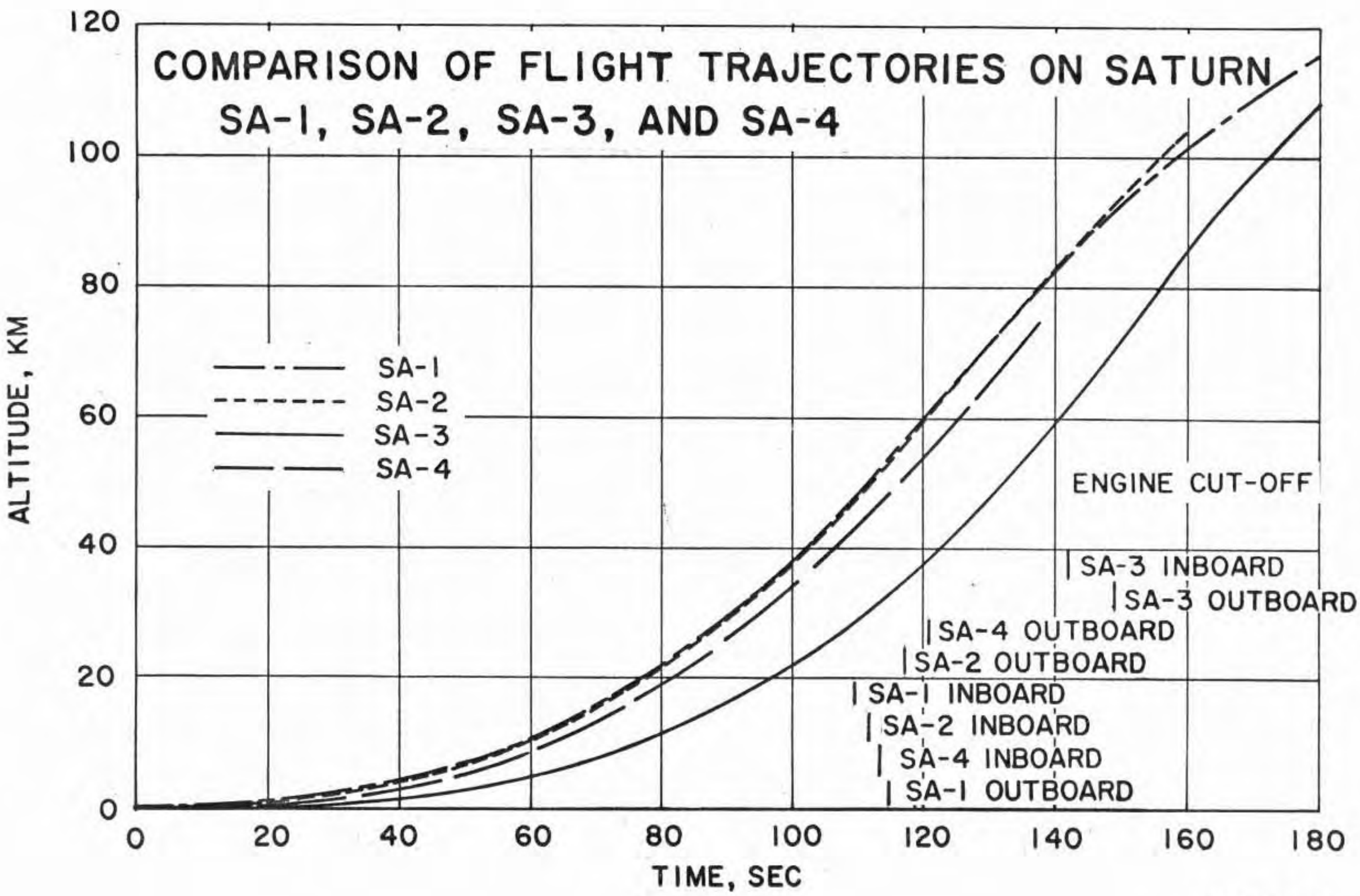
COMPARISON OF FLIGHT TRAJECTORIES ON SATURN
SA-1, SA-2, SA-3, AND SA-4
ALTITUDE, KM
TIME, SEC
SA-1
SA-2
SA-3
SA-4
ENGINE CUT-OFF
SA-3 INBOARD
SA-3 OUTBOARD
SA-4 OUTBOARD
SA-2 OUTBOARD
SA-1 INBOARD
SA-2 INBOARD
SA-4 INBOARD
SA-1 OUTBOARD
0
20
40
60
80
100
120
0
20
40
60
80
100
120
140
160
180

FIGURE 2

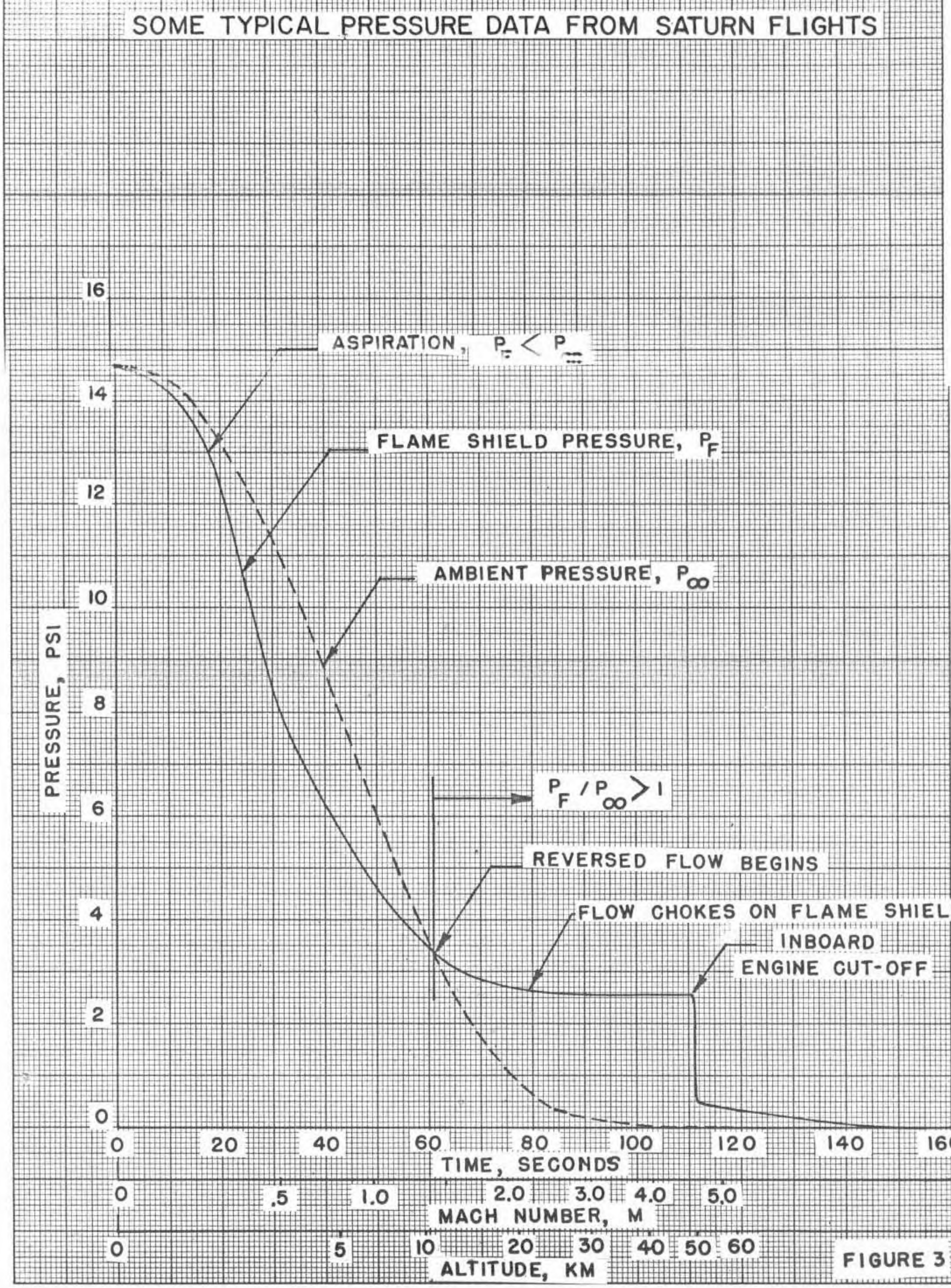

SOME TYPICAL PRESSURE DATA FROM SATURN FLIGHTS
PRESSURE, PSI
0
2
4
6
8
10
12
14
16
ASPIRATION, $P_F < P_\infty$
FLAME SHIELD PRESSURE, P_F
AMBIENT PRESSURE, P_∞
$P_F / P_\infty > 1$
REVERSED FLOW BEGINS
FLOW CHOKES ON FLAME SHIELD
INBOARD
ENGINE CUT-OFF
0 20 40 60 80 100 120 140 160
TIME, SECONDS
0 .5 1.0 2.0 3.0 4.0 5.0
MACH NUMBER, M
0 5 10 20 30 40 50 60
ALTITUDE, KM

FIGURE 3

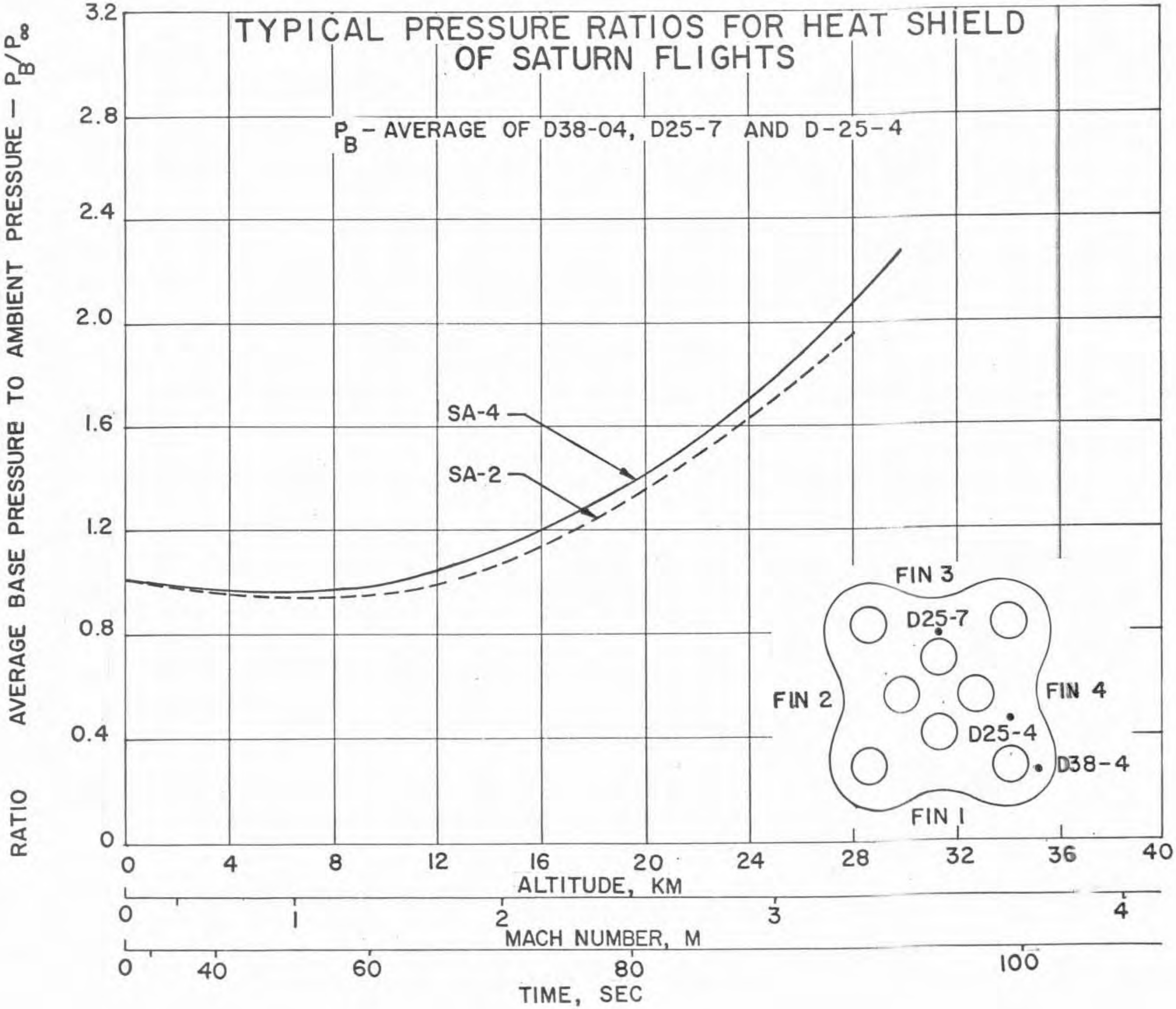
TYPICAL PRESSURE RATIOS FOR HEAT SHIELD
OF SATURN FLIGHTS
P_B - AVERAGE OF D38-04, D25-7 AND D-25-4
RATIO AVERAGE BASE PRESSURE TO AMBIENT PRESSURE — P_B/P_∞
SA-4
SA-2
FIN 1
FIN 2
FIN 3
FIN 4
D25-7
D25-4
D38-4
ALTITUDE, KM
MACH NUMBER, M
TIME, SEC

FIGURE 4

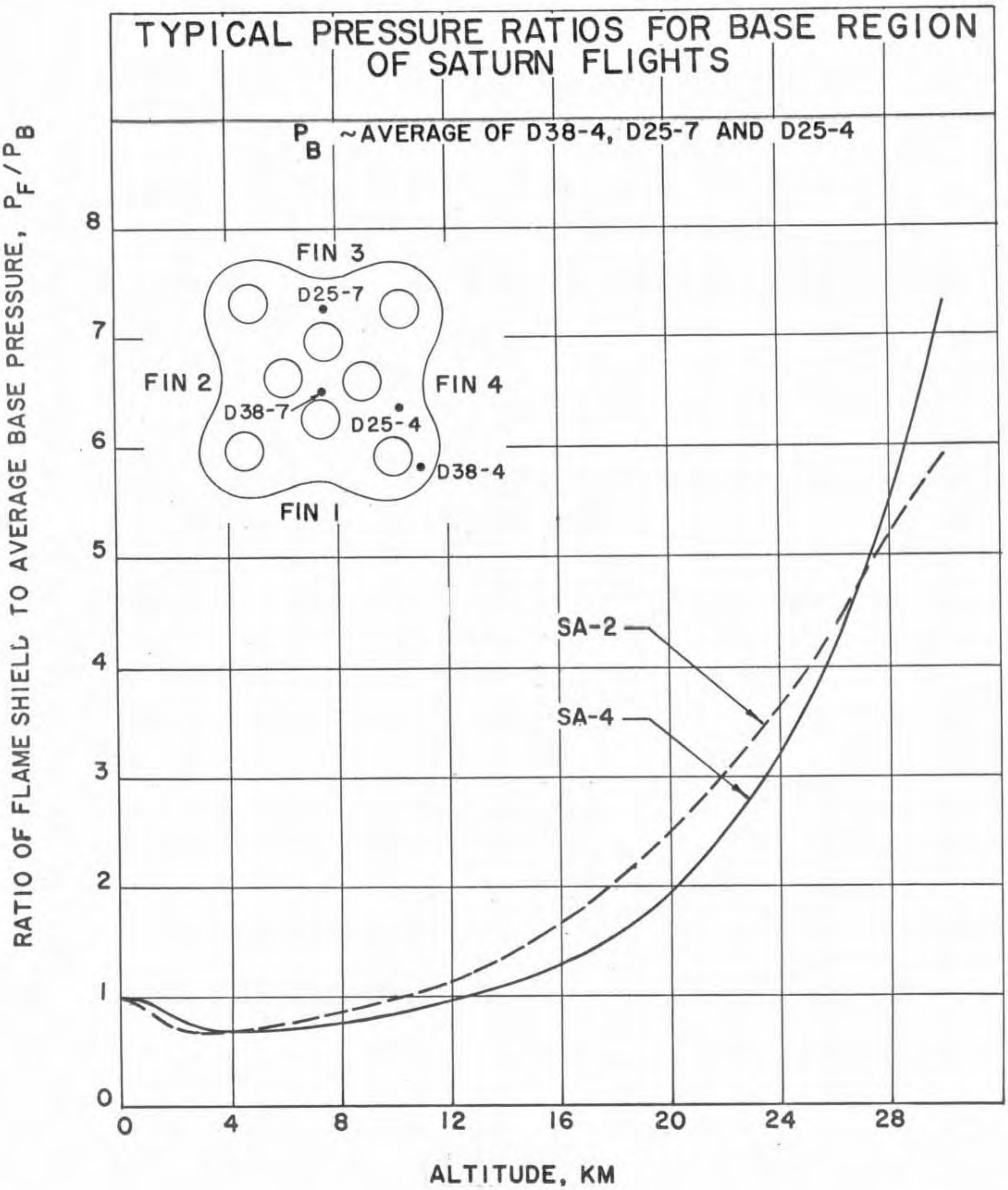
TYPICAL PRESSURE RATIOS FOR BASE REGION OF SATURN FLIGHTS
P_B ~AVERAGE OF D38-4, D25-7 AND D25-4
FIN 3
FIN 2
FIN 4
FIN 1
D25-7
D38-7
D25-4
D38-4
SA-2
SA-4
RATIO OF FLAME SHIELD TO AVERAGE BASE PRESSURE, P_F/P_B
ALTITUDE, KM
0
1
2
3
4
5
6
7
8
0
4
8
12
16
20
24
28

FIGURE 5

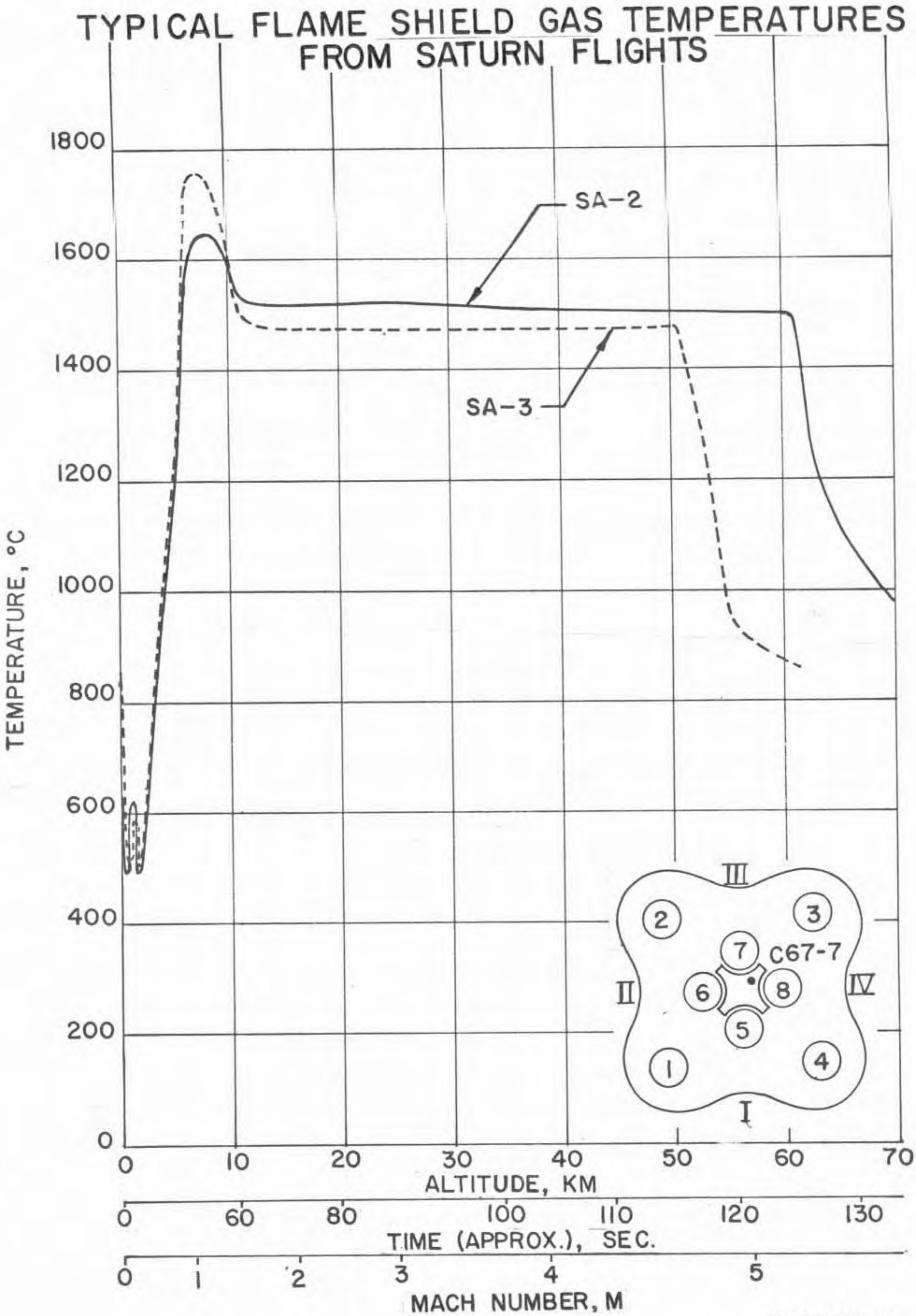
TYPICAL FLAME SHIELD GAS TEMPERATURES
FROM SATURN FLIGHTS
SA-2
SA-3
TEMPERATURE, °C
1800
1600
1400
1200
1000
800
600
400
200
0
III
II
IV
I
1
2
3
4
5
6
7
8
C67-7
0
10
20
30
40
50
60
70
ALTITUDE, KM
0
60
80
100
110
120
130
TIME (APPROX.), SEC.
0
1
2
3
4
5
MACH NUMBER, M

FIGURE 6

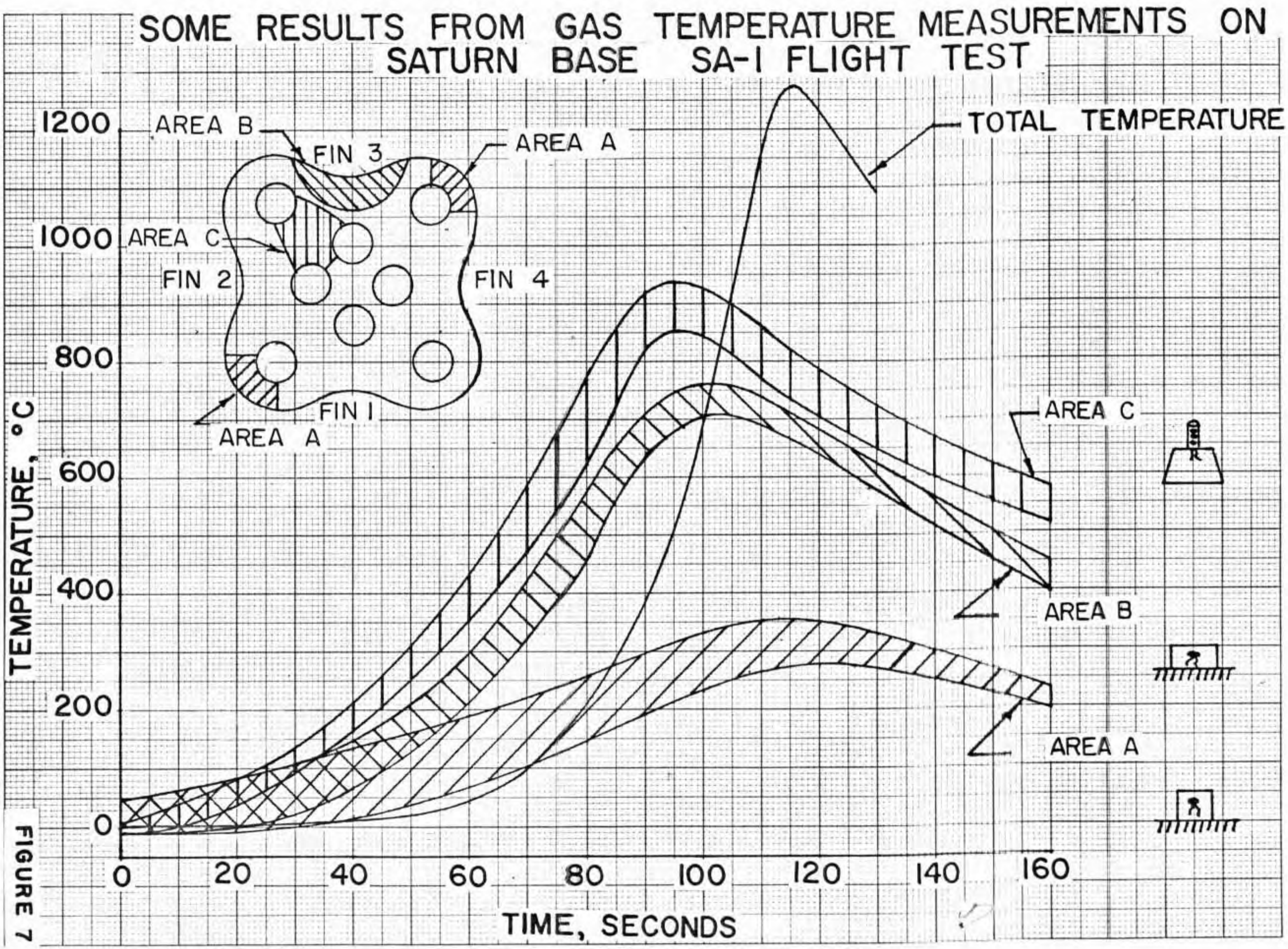
SOME RESULTS FROM GAS TEMPERATURE MEASUREMENTS ON
SATURN BASE SA-1 FLIGHT TEST
TOTAL TEMPERATURE
AREA B
AREA A
FIN 3
AREA C
FIN 2
FIN 4
FIN 1
AREA A
AREA C
AREA B
AREA A
TEMPERATURE, °C
1200
1000
800
600
400
200
0
0
20
40
60
80
100
120
140
160
TIME, SECONDS

FIGURE 7

SOME TYPICAL SATURN FLIGHT TEST DATA TOTAL AND RADIATION HEATING AS A FUNCTION OF ALTITUDE ON THE HEAT SHIELD

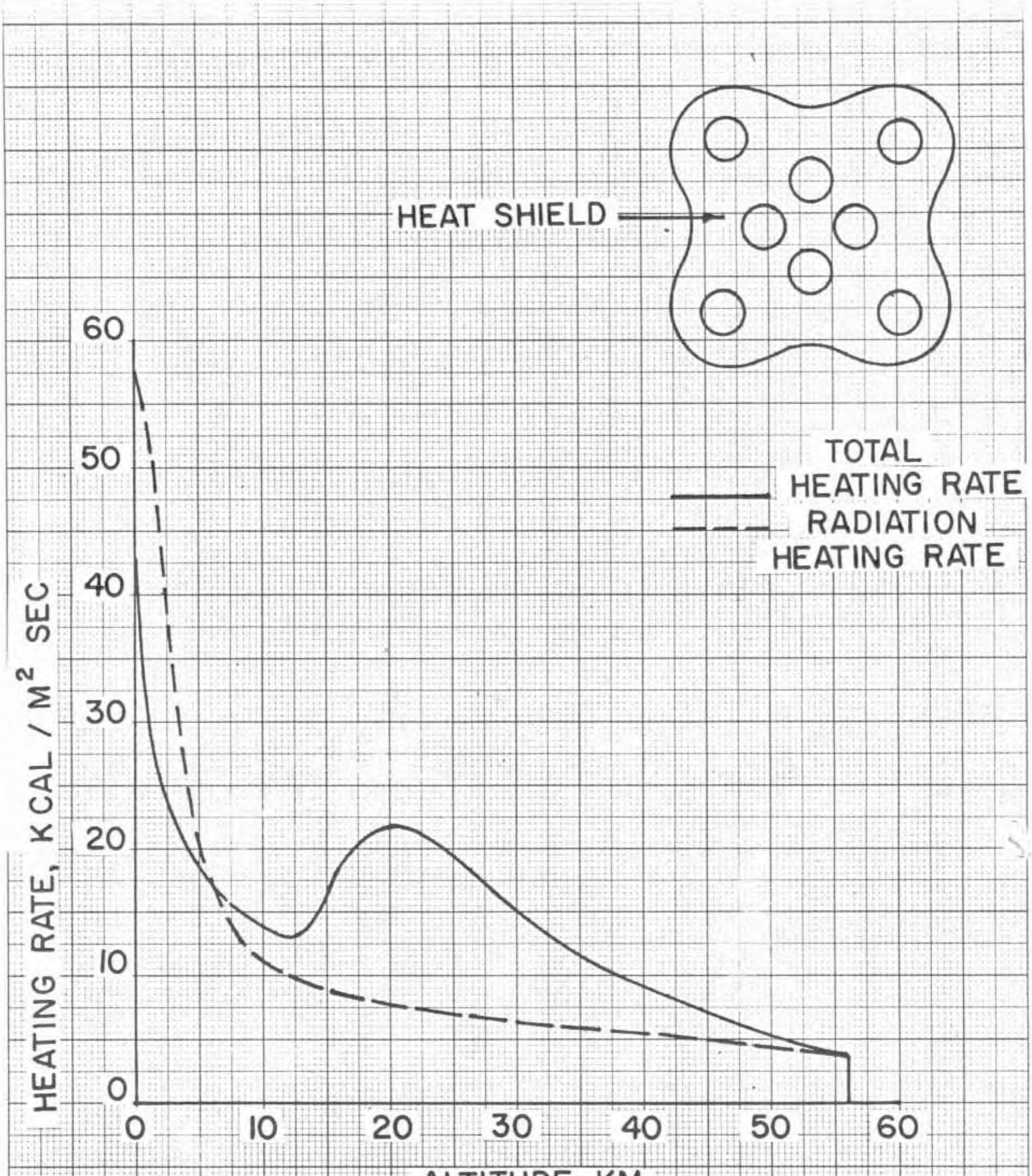

FIGURE 8

CONSTANT PRESSURE COMBUSTOR

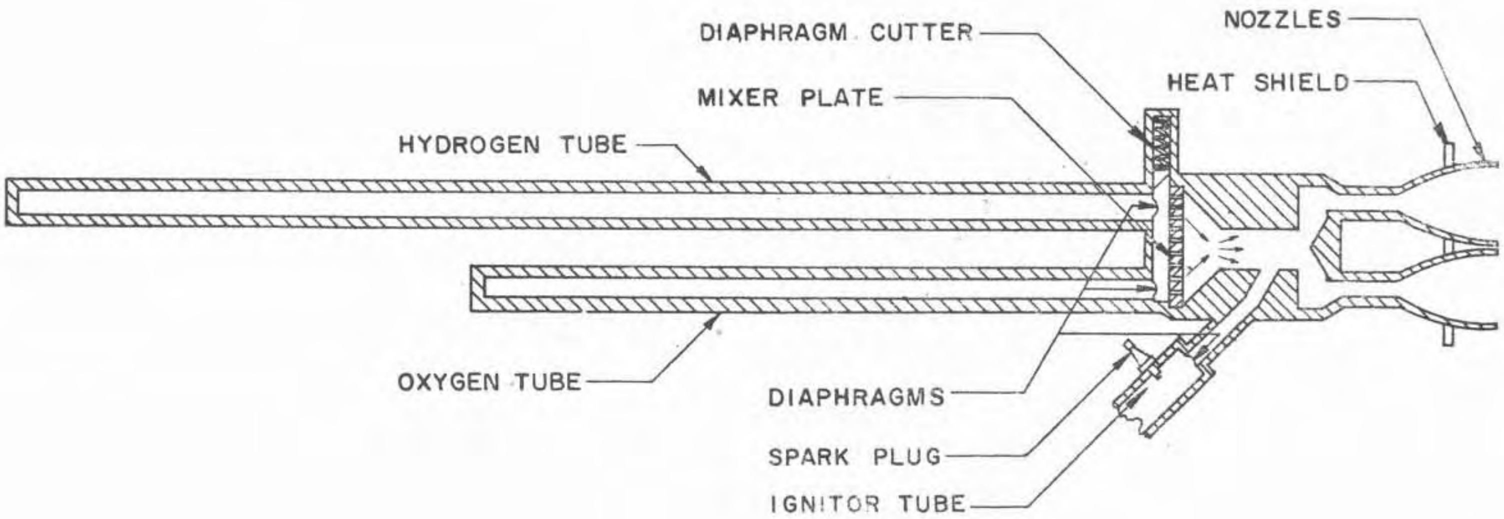

FIGURE 9

CONSTANT PRESSURE COMBUSTOR MOUNTED IN 13' DIAMETER VACUUM TANK AT CORNELL AERONAUTICAL LABORATORY

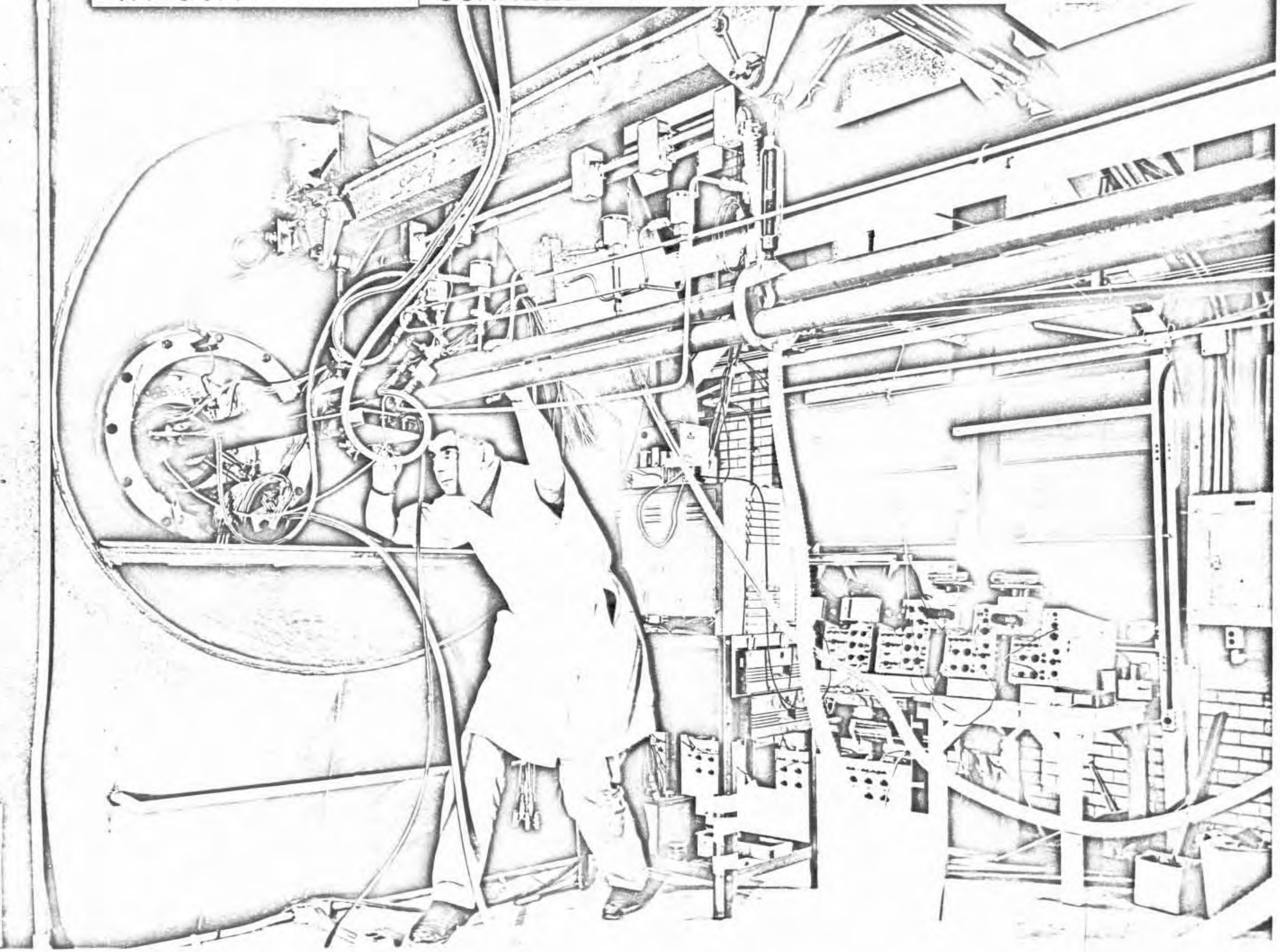

FIGURE 10

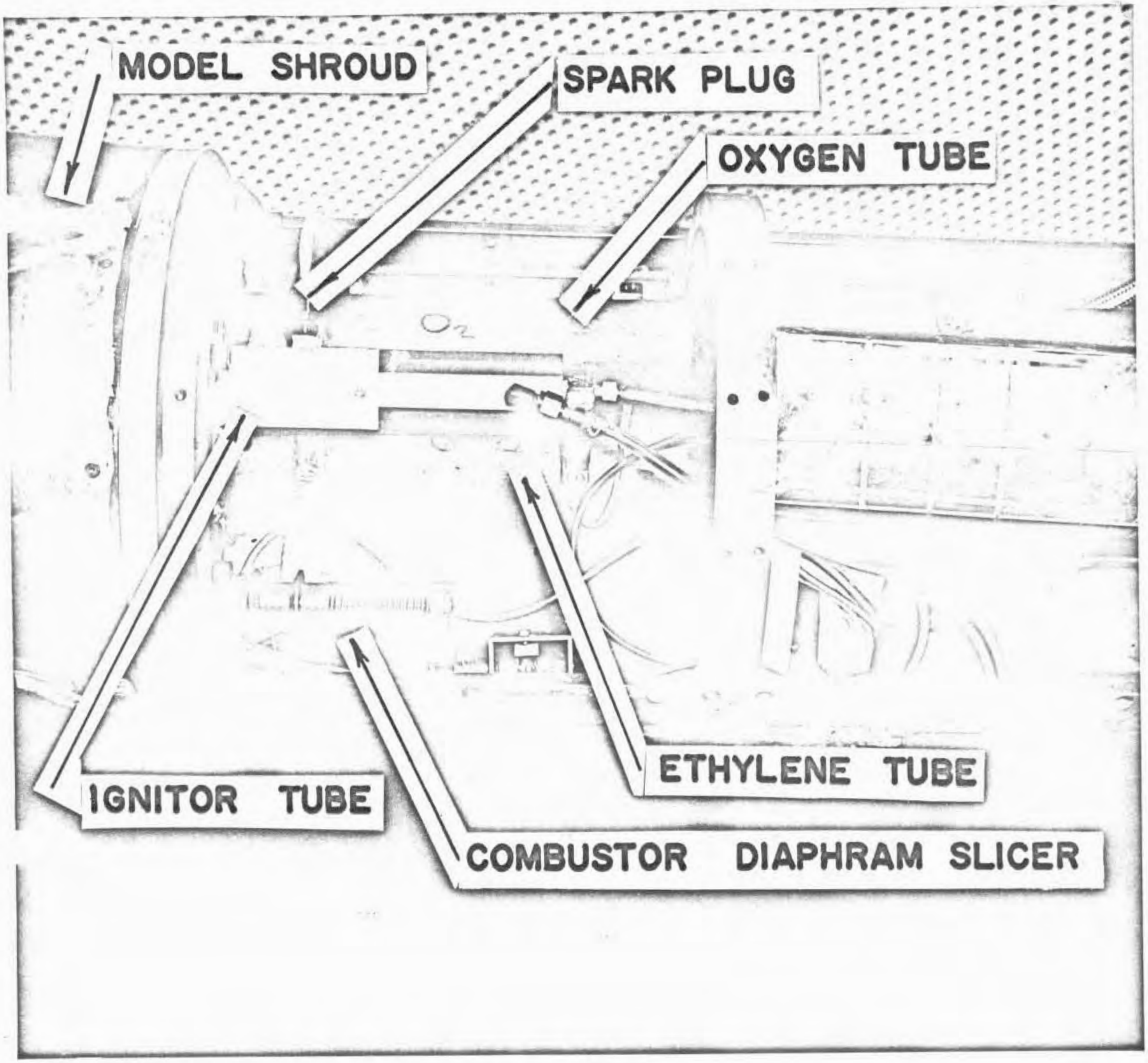

CORNELL SA-1 0.0547 SCALE MODEL
CONSTANT PRESSURE COMBUSTOR

FIGURE 10a

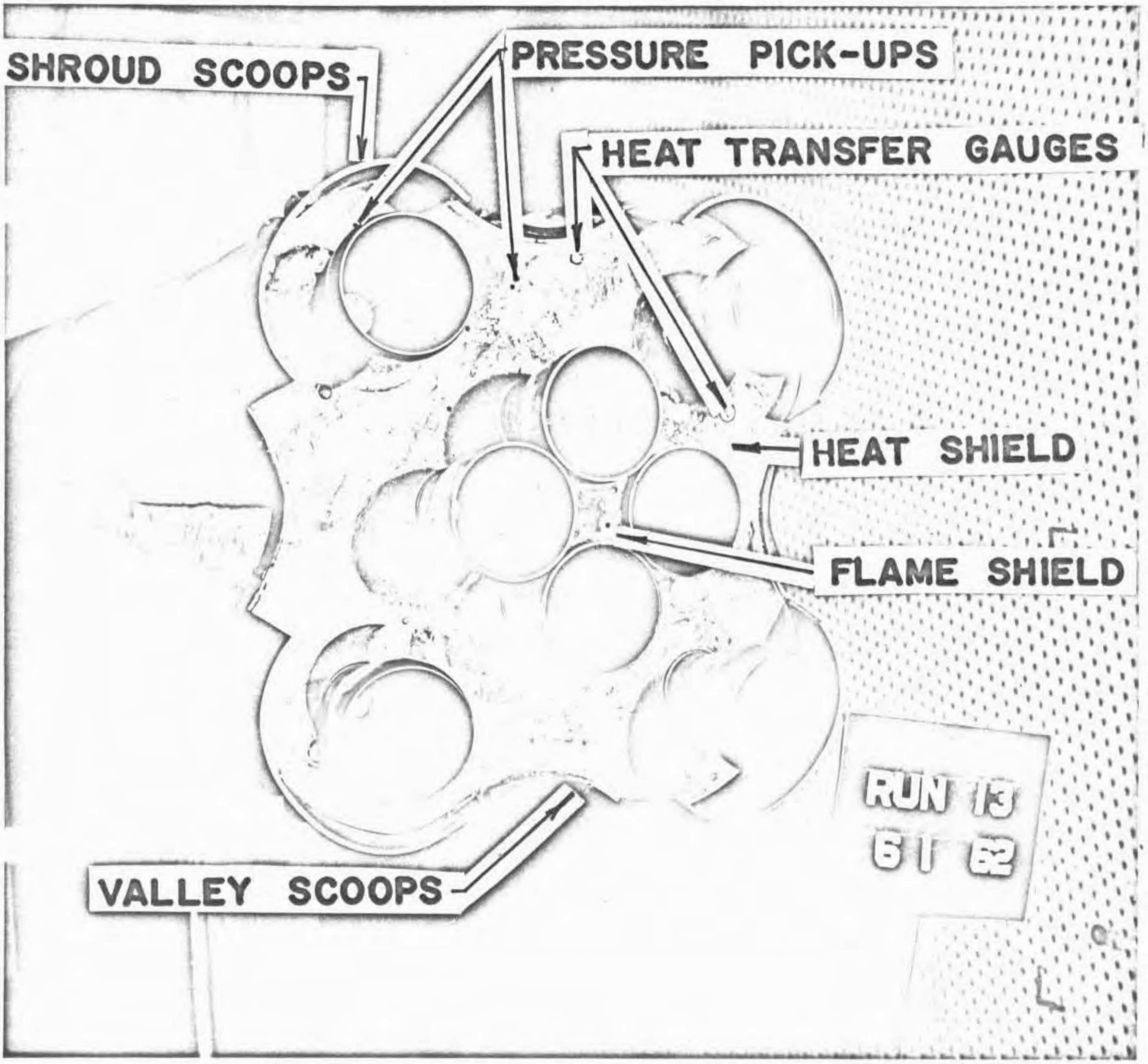

CORNELL SA-1 0.0547 SCALE MODEL
LOCATED IN 8' X 8' TRANSONIC TUNNEL

FIGURE 10b

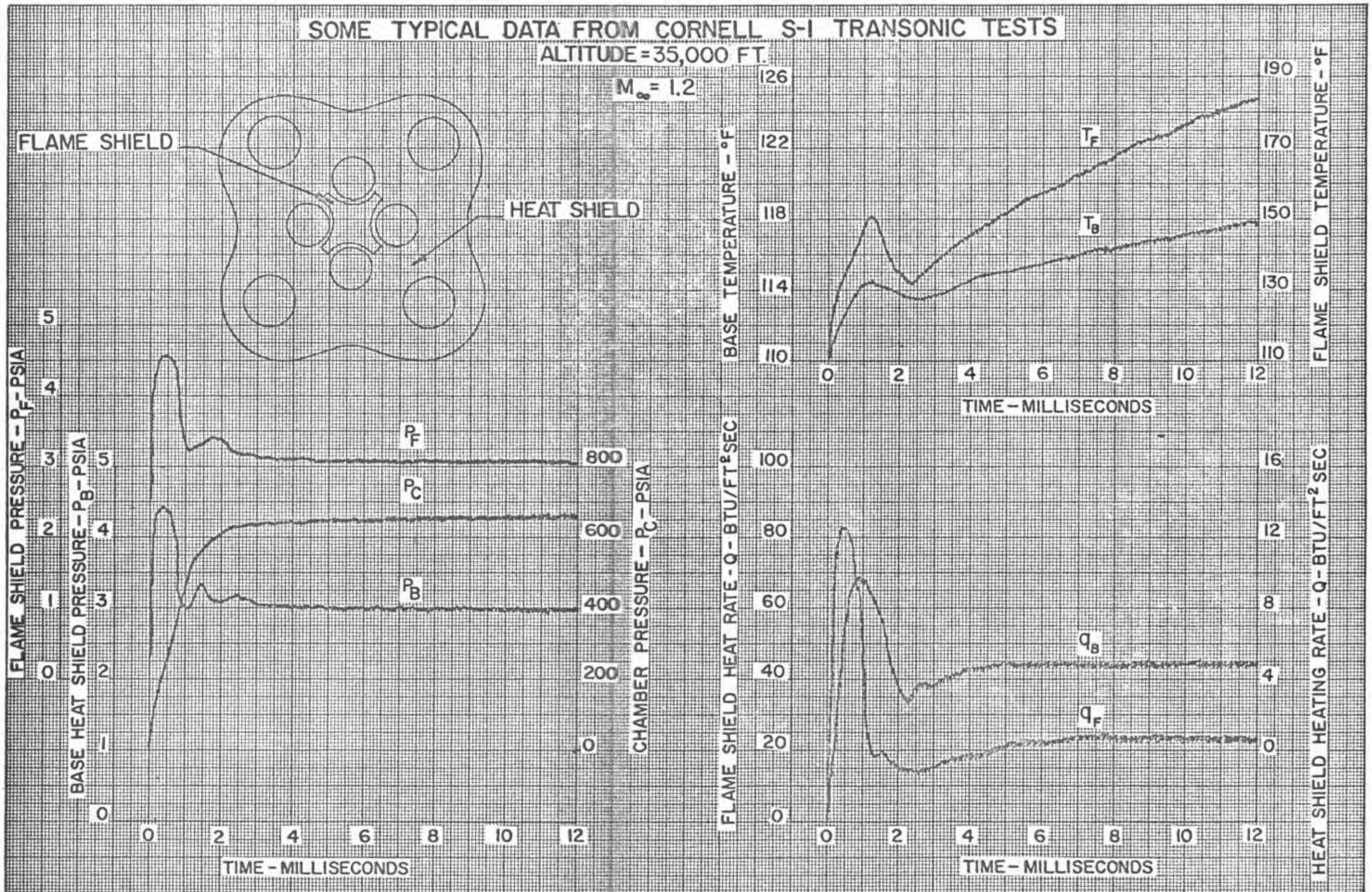
SOME TYPICAL DATA FROM CORNELL S-I TRANSONIC TESTS
ALTITUDE = 35,000 FT.
M_∞ = 1.2
FLAME SHIELD
HEAT SHIELD
FLAME SHIELD PRESSURE - P_F - PSIA
BASE HEAT SHIELD PRESSURE - P_B - PSIA
CHAMBER PRESSURE - P_C - PSIA
P_F
P_C
P_B
TIME - MILLISECONDS
BASE TEMPERATURE - °F
FLAME SHIELD TEMPERATURE - °F
T_F
T_B
TIME - MILLISECONDS
FLAME SHIELD HEAT RATE - Q - BTU/FT² SEC
HEAT SHIELD HEATING RATE - Q - BTU/FT² SEC
q_B
q_F
TIME - MILLISECONDS
FIGURE 11

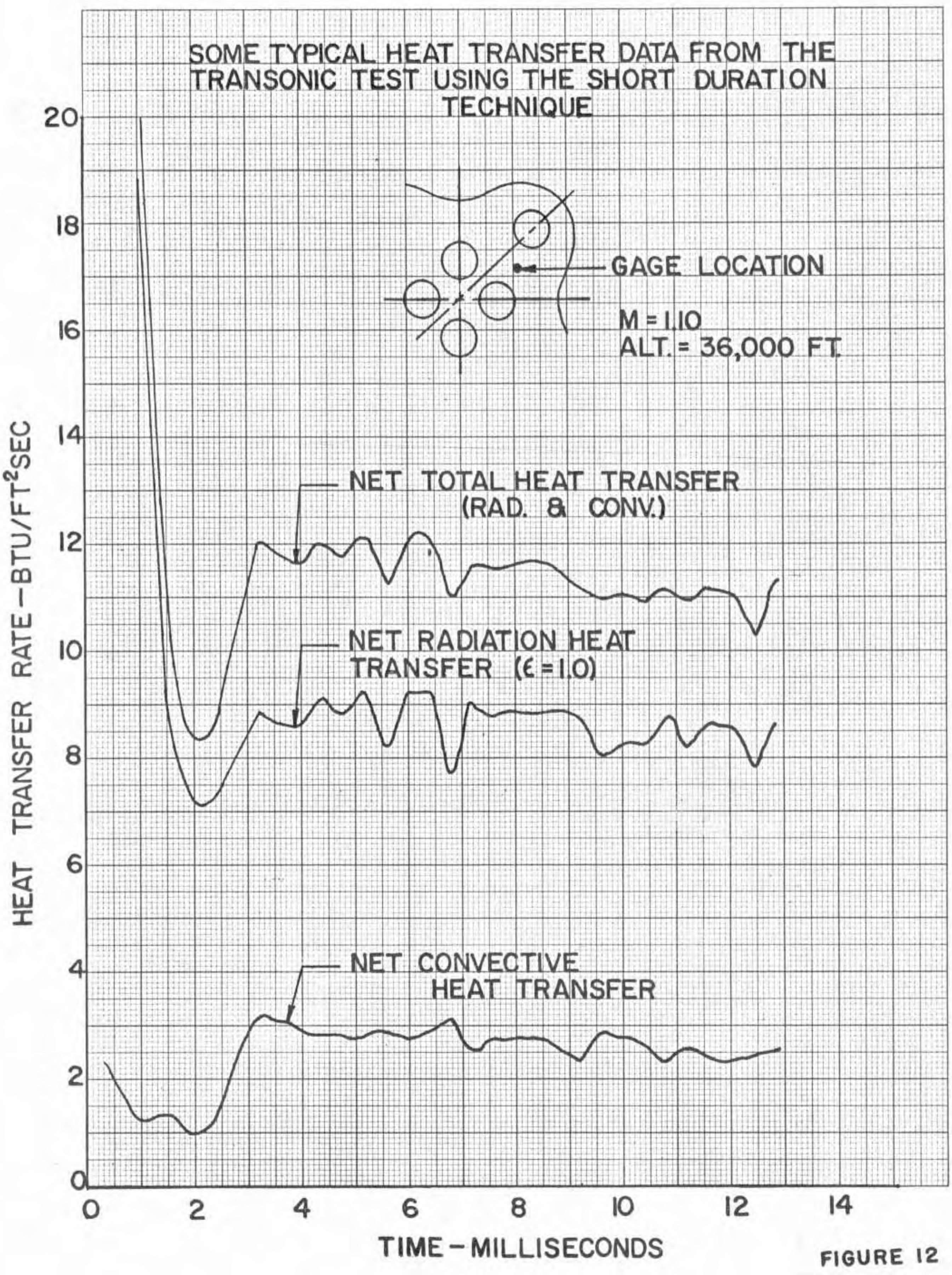
SOME TYPICAL HEAT TRANSFER DATA FROM THE TRANSONIC TEST USING THE SHORT DURATION TECHNIQUE
GAGE LOCATION
M = 1.10
ALT. = 36,000 FT.
NET TOTAL HEAT TRANSFER (RAD. & CONV.)
NET RADIATION HEAT TRANSFER (ε = 1.0)
NET CONVECTIVE HEAT TRANSFER
HEAT TRANSFER RATE – BTU/FT²SEC
TIME – MILLISECONDS
0
2
4
6
8
10
12
14
16
18
20

FIGURE 12

CORNELL SATURN S-I TRANSONIC BASE HEATING TEST
RESULTS COMPARED WITH LONG DURATION MODEL TESTS

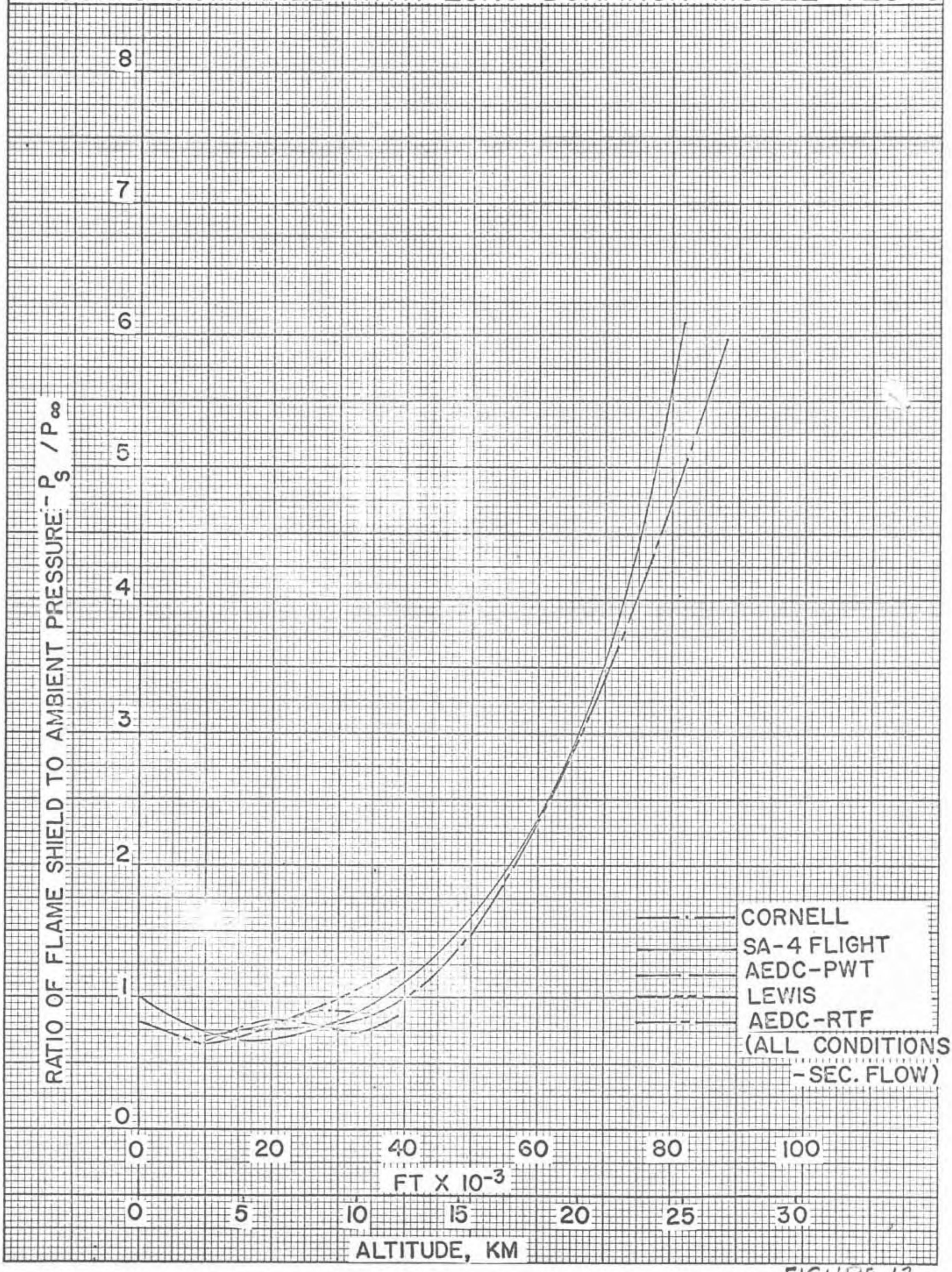

FIGURE 13

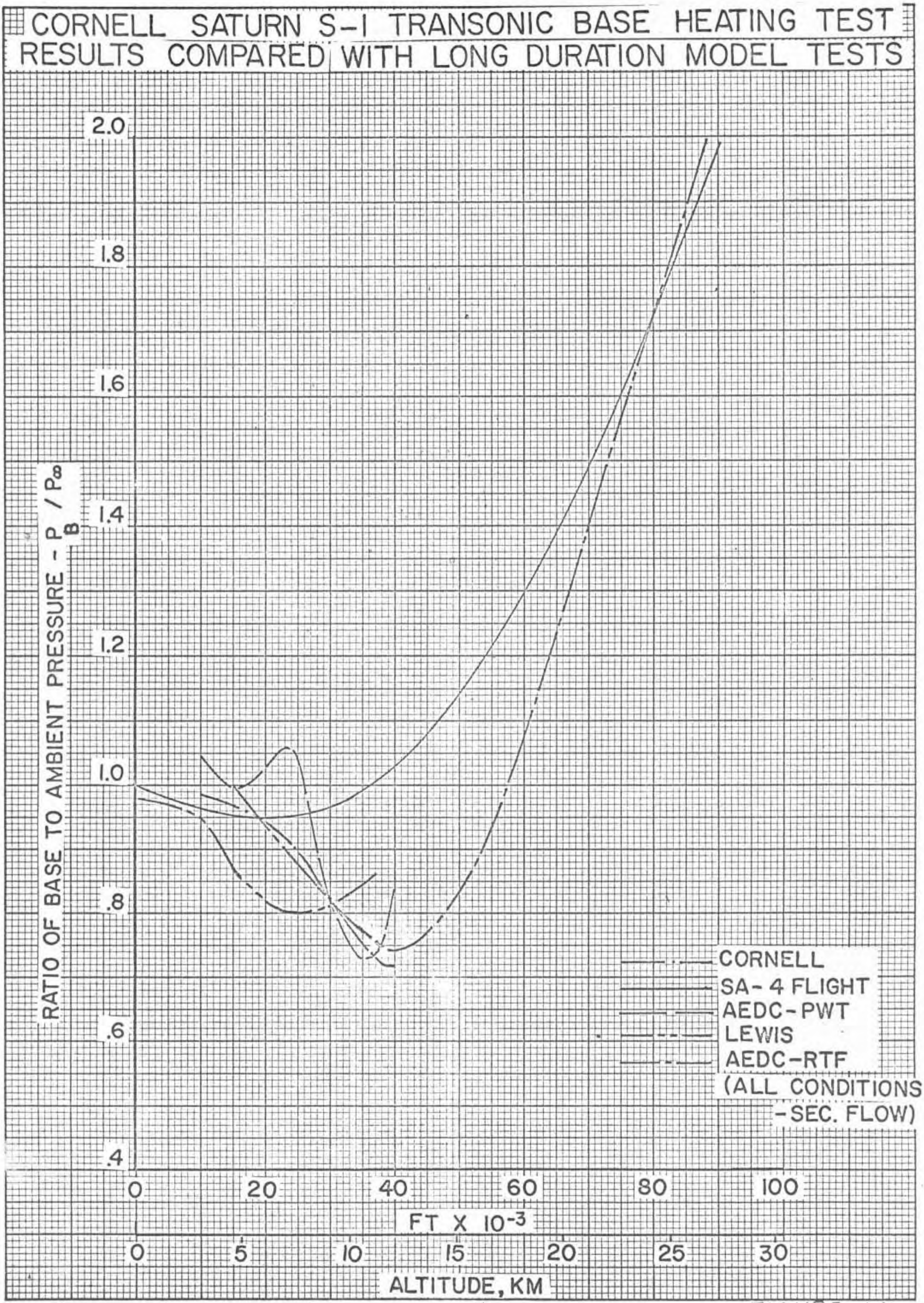
CORNELL SATURN S-I TRANSONIC BASE HEATING TEST RESULTS COMPARED WITH LONG DURATION MODEL TESTS
RATIO OF BASE TO AMBIENT PRESSURE - P_B / P_∞
2.0
1.8
1.6
1.4
1.2
1.0
.8
.6
.4
0
20
40
60
80
100
FT X 10^{-3}
0
5
10
15
20
25
30
ALTITUDE, KM
CORNELL
SA-4 FLIGHT
AEDC-PWT
LEWIS
AEDC-RTF
(ALL CONDITIONS -SEC. FLOW)

FIGURE 14

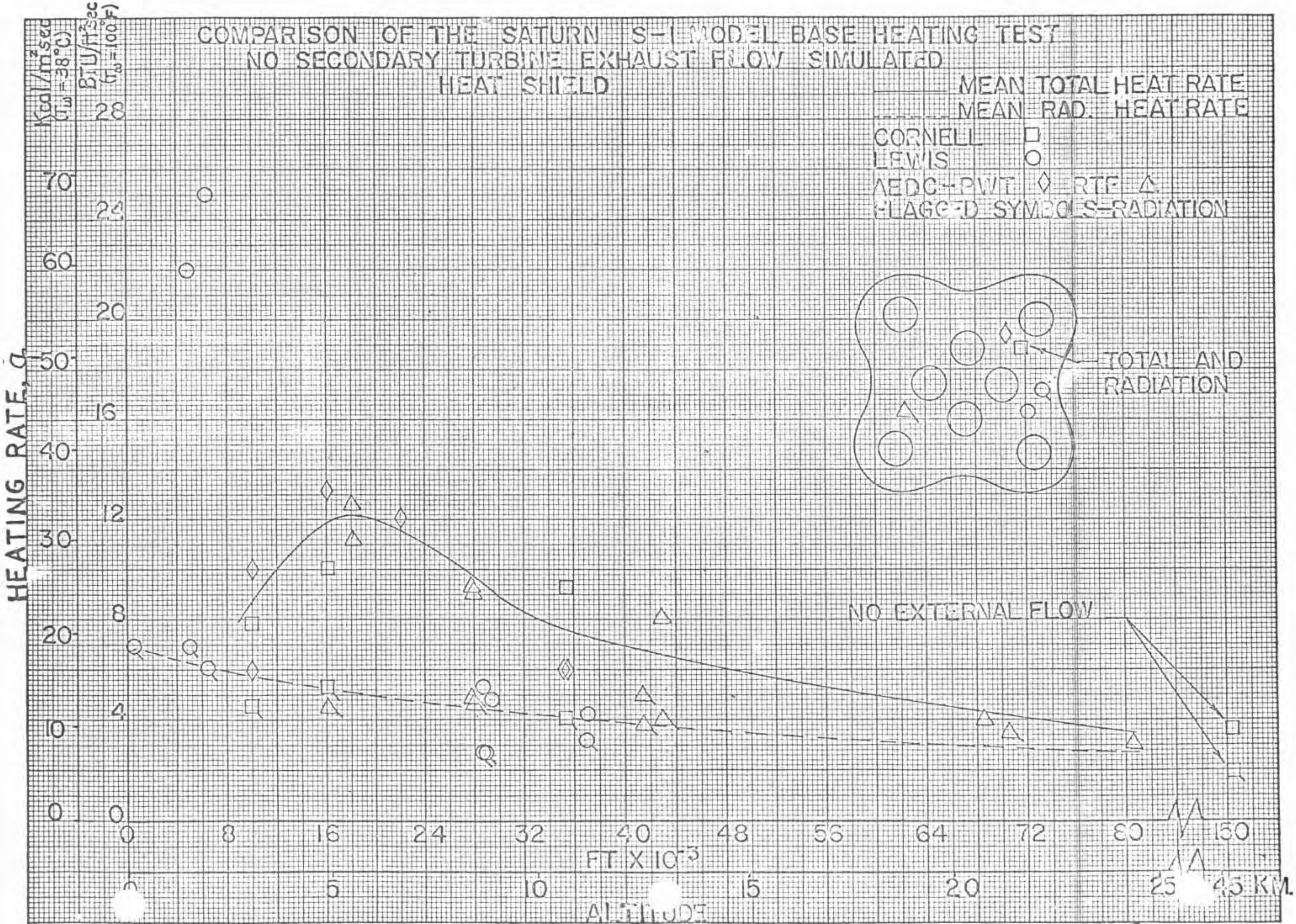
COMPARISON OF THE SATURN S-I MODEL BASE HEATING TEST
NO SECONDARY TURBINE EXHAUST FLOW SIMULATED
HEAT SHIELD
MEAN TOTAL HEAT RATE
MEAN RAD. HEAT RATE
CORNELL
LEWIS
AEDC-PWT
RTF
FLAGGED SYMBOLS=RADIATION
TOTAL AND RADIATION
NO EXTERNAL FLOW
Kcal/m²sec (T_w=38°C)
BTU/ft²sec (T_w=100°F)
HEATING RATE, q
FT X 10³
ALTITUDE
KM.

FIGURE 15